*Thermophysics and Aeromechanics*, *2001*, *Vol. 8*, *No. 3*

UDC 621.362.537.84

# NUMERICAL MODELING OF OPERATION OF HIGH-PRESSURE DETONATION MHD-GENERATOR*

**V.V. DEREVYANKO**

*Institute of Numerical Modeling SB RAS*, *Krasnoyarsk*, *Russia*

(*Received March 26*, *2001*)

The numerical modeling of the operation of a detonation MHD generator with T-layer has been performed at large pressures in the duct. It is shown that the radiation absorption inside the T-layer leads to a considerable variation of the layer characteristics, increase in the specific power and generator efficiency.

## INTRODUCTION

As was shown in [1], at the duct pressures $P \geq 100$ atm. the effect of radiation choking is manifested in the $T$-layer of the detonation MHD generator. In this connection, a correct consideration of both radiation and absorption in the flow are needed. An analysis of the operation of detonation MHD generator with $T$-layer at a small pressure in the flow has shown that the $T$-layer motion velocity behind the detonation wave front is small in the constant section duct and decreases as the wave propagates along the channel. Therefore, we have considered in the present computation a variable section duct enabling one to increase the flow velocity. In the previous model of the detonation MHD generator the loading coefficient was assumed to be constant, what was acceptable for preliminary computations. However, while passing to large pressures the initiation energy increases proportionally to the pressure increase. In this connection, the use of the flow energy for the heating of $T$-layer is well justified. An intense heating of the latter is possible at small loading coefficients, whereas it is necessary to increase it for increasing the energy production and efficiency. This seeming contradiction is quite solvable if the loading coefficient increases at the $T$-layer heating. Such a regime can be realized when using a constant loading resistance. This is more justified also from the viewpoint of the design of the electric scheme of the MHD duct, because in this case the condition of the absence of the voltage gradient along the continuous conductive electrodes is satisfied. The gas dynamic flow characteristics at large temperature and pressure gradients naturally depend very strongly on the local molecular mass and the adiabatic exponent. The ideal solution would be the use of the real gas model. However, at the given stage with regard for problem complexity one had to restrict oneself to the politropic gas model, that is to compute the local molecular mass, and to assume the adiabatic exponent to be constant. Its value was determined from the analysis of the $\gamma(p, T)$ dependence in the operation range of the pressure and temperature variation. The

* The work was supported financially by the SB RAS integration project No. 03 “The Development and Validation of Scramjet Model with Magnetohydrodynamic Flow Control in Combustion Chamber”.

task of the optimization of the generator power characteristics was not posed in the present work. The main attention was paid to the analysis of the pressure effect on flow characteristics for the purpose of determining the direction of further research.

## 1. COMPUTATIONAL MODEL

In the present work, a number of changes have been introduced in the MHD generator model [1]. The possibility of conducting the computations for the variable section duct has been firstly added. Secondly, the approach to the computation of radiation losses in the *T*-layer has been changed: also the absorption processes are now taken into account besides the radiation processes, which enables us to model the radiation choking in *T*-layer. The approximation of a constant loading coefficient is thirdly replaced with a more realistic model of a constant loading resistance, which has enabled us to model more exactly the processes of the *T*-layer initiation and its interactions with the magnetic field.

### 1.1. The system of gas dynamics equations

The general system of gas dynamics equations governing the gas dynamics in the duct of a detonation MHD generator is as follows:

$$\frac{\partial AU}{\partial t} + \frac{\partial AF}{\partial x} = S \ ,$$

$$U = (\rho,\ m,\ E)^{\mathrm{T}} \ ,$$

$$F = \left(m,\ m^2/\rho + p,\ (E+p)m^2/\rho\right)^{\mathrm{T}}$$ (была лишняя формула)

$$S = \begin{pmatrix} 0 \\ A\left(JB + p\dfrac{\partial A}{\partial x}\right) \\ A(Q_R - Q_{\mathrm{load}} + Q_{\mathrm{ini}} + Q_{\mathrm{det}}) \end{pmatrix},$$

where $A$ is the duct cross-section area, ρ, $m$ and $E$ are the conservative variables: the density, momentum and energy, $p$ is the pressure; $Q_R$, $Q_{\mathrm{load}}$, $Q_{\mathrm{ini}}$, and $Q_{\mathrm{det}}$ are the energy sources: the radiation losses, the energy released at the loading, the initiation energy and the heat release in detonation wave; $J$ is the current in the chain *T*-layer — loading; $B$ is the magnetic induction. The superscript T denotes the transposition.

The ideal politropic gas equation of state with a constant adiabatic exponent $\gamma = \mathrm{const}$ and molecular mass $\mu = \mu(p, T)$ given in tabular form were used in the model.

### 1.2. Radiation transfer

The one-dimensional equation of radiation transfer for a plane layer may be presented as

$$\mu \frac{dI_\nu}{dx} + \chi_\nu I_\nu = 2\pi\chi_\nu I_{\nu p}, \quad x_0 \le x \le x_1,\ -1 \le \mu \le 1, \tag{1}$$

where $I_\nu$ is the spectral intensity of radiation, ν is the photon frequency, μ is the cosine of the angle between the direction of photon motion and the $x$ — axis, $\chi_\nu$ is the coefficient of photons absorption with frequency ν corrected by the forced radiation, $I_{\nu p}$ is the spectral intensity of equilibrium radiation equal to

$$I_{\nu p} = \frac{2h\nu^3}{c^2(\exp\{h\nu/kT\}-1)}.$$

Having solved the equation and found the distribution of the radiation spectral intensity one can find the flux and density of the radiation energy as well as the radiation losses from the unit volume:

$$H = \int_0^\infty d\nu \int_{-1}^{1} \mu\, I_k\, d\mu,\ \ U = \frac{1}{c}\int_0^\infty d\nu \int_{-1}^{1} I_k\, d\mu,\ \ Q_R = -\mathrm{div} H .$$

Equation (1) was solved by the multi-group approximation [3]. The overall frequency spectrum involved was partitioned into $N_\nu$ intervals of groups. In each group the absorption coefficient was found with the aid of averaging after Planck:

$$\chi_k = \int_{\nu_k}^{\nu_{k+1}} \chi(\nu) I_{\nu p}\, d\nu \Bigg/ \int_{\nu_k}^{\nu_{k+1}} I_{\nu p}\, d\nu$$

and assumed to be independent of frequency. Equation (1) can be written in this case as a system of multi-group equations, and each of them is solved independently:

$$\mu \frac{dI_k}{dx} + \chi_k I_k = 2\chi_k \sigma_k T^4,\ \ 1 \le k \le N_\nu, \tag{2}$$

where

$$\sigma_k(T) = \frac{2\pi k^4}{c^2 h^3}\left[\tilde{\sigma}\left(\frac{h\nu_{k+1}}{kT}\right) - \tilde{\sigma}\left(\frac{h\nu_k}{kT}\right)\right],$$

$$\tilde{\sigma}(x) = \int_0^x \frac{\zeta^3}{e^\zeta - 1} d\zeta .$$

In this case, the flux and the radiation energy density can be presented as

$$H = \sum_0^{N_\nu} \int_{-1}^{1} \mu\, I_k\, d\mu,\ \ U = \frac{1}{c}\sum_0^{N_\nu} \int_{-1}^{1} I_k\, d\mu .$$

The boundary conditions for equation (2) were chosen as the conditions of the absence of radiation incident outside [3]:

$$I_\nu(\mu, \nu) = 0 \text{ (to the left and to the right).}$$

The obtained system of equations was solved numerically by a difference scheme taken from [3], which has the second order of approximation on smooth solutions.

### 1.3. Distribution of the current density in *T*-layer

The interaction of *T*-layer with magnetic field was calculated previously in the model of detonation MHD generator in the approximation of constant loading coefficient.

$$K = \frac{\Delta U(x)}{\varepsilon(x)} = \text{const} \ ,$$

where $\Delta U$ is the voltage on the loading, $\varepsilon = u(x)B$ is the electric field strength. If we denote the loading resistance by $R^L$, the resistance of the *T*-layer by $R^T$, then the loading coefficient may be written as

$$K = \frac{R^L(x)}{R^L(x) + R^T(x)} .$$

The equality is satisfied only in the case of an ideally sectioned MHD-duct, and a specific loading resistance corresponds to each region of the *T*-layer. It is impossible to implement such a loading scheme in an actual generator. The model of a constant loading coefficient was, therefore, modified to the model of a constant loading resistance. In this case, the generator electrodes are continuous and ideally conductive (there is no potential gradient along the electrodes) and are loaded for a constant resistance $R^L$. Such a scheme is more preferable for the *T*-layer development, because at the initial development stage of the *T*-layer, its integral resistance is much larger than the loading resistance, and the loading coefficient is close to zero. Therefore, at the initial moment of time nearly all the energy generated is spent for the heating of *T*-layer, and it develops quickly.

For continuous electrodes and constant loading resistance $\Delta U = JR^L$. According to the Ohm's law for a complete chain, the current density in the *T*-layer may be written as

$$J(x) = \frac{\varepsilon(x) - JR^L}{R^T(x)} , \tag{3}$$

where $\varepsilon(x) = u(x)A(x)B$ is the electric field strength. One can determine the resistance of a *T*-layer (*T* курсивом) interval with length $h$ knowing the gas conductivity $\sigma(p, T)$ and the duct cross-section $Y$:

$$R^T(x) = \frac{A(x)}{\sigma(p(x),\, T(x))hY} .$$

The integration of equation (3) over the total region of the *T*-layer $\Delta l$ yields the expression for the total current:

$$J = \left(1 + R^L\right) \int_{\Delta l} \frac{\varepsilon(x)}{R^T(x)} dx \int_{\Delta l} \frac{1}{R^T(x)} dx .$$

The power released in the loading, and the Joulean dissipation power may be written, respectively, as

$$Q_{\text{load}} = \int_{\Delta l} J(x) JR^L(x) dx, \ \ Q_{\text{dis}} = \int_{\Delta l} J(x) JR^T(x)\, dx .$$

## 2. RESULTS OF NUMERICAL EXPERIMENTS

For a preliminary estimation of the operating regime of high and low pressure generators we have carried out an analysis of the radiation characteristics of combustion products of an air-hydrogen mixture from the *T*-layer with a sinusoidal temperature profile versus the pressure and the layer dimensions [4]. From the analysis of the dependencies obtained, the operating pressures in gas flow and the initial pressures $p_0$ of the working mixture in the detonation combustion chamber were chosen.

For the high-pressure generator, the range of operating pressures made 100 — 300 atm and the initial pressure $p_0$ = 30 atm. In the low pressure generator $p_0$ = 0.5 atm., the flow pressure amounts to 2 — 5 atm. The following integral quantities and their dependencies on time were determined in the numerical modeling: $E_{\text{int}}$ (пробел перед E), the internal energy in the duct, $E_{\text{det}}$, the energy of fuel burnt, $E_{\text{ini}}$, the energy of the *T*-layer initiation, $E_{\text{dis}}$, the Joulean dissipation energy in the *T*-layer, $E_L$, the energy released on the loading, $E_R$, the energy of rdiation from *T*-layer, $E_{\text{out}}$, the flow energy at the duct outlet to diffuser, *J* the total current in the loading, *K*, the effective loading coefficient, $\Delta l$, the total dimension of the *T*-layer determined at the temperature level $T = 7 \cdot 10^3$ K, $\eta_{\text{el}} = (E_L - E_{\text{ini}})/E_{\text{det}}$, the electric efficiency, $E_{\text{layer}}$, the internal energy of the *T*-layer, $W_L$, the specific power capacity of the generator.

The energy balance was computed for the check-up at each moment of time, which was determined as

$$\frac{E_{\text{int}}(0) + E_{\text{det}} + E_{\text{ini}}}{E_L(t) + E_R(t) + E_{\text{int}}(t) + E_{\text{out}}(t)} = \text{const} .$$

It is to be noted that the energy balance is conserved with an error 2 %, which agrees with the accuracy of the chosen numerical methods.

We present below a comparative analysis of two numerical experiments conducted for the high and low pressure generators. The generator scheme is given in Fig. 1. The detonation chamber 1.5 m in length and 2 m in height was filled with a stoichiometric mixture of hydrogen and air with heat release 3.5 kJ/kg and the adiabatic exponent 1.35, at pressure $p_0$ and room temperature. The detonation wave was initiated on the left side of the chamber. A planar nozzle 0.5 m in height was modeled as profiled one for a correct operation of numerical methods. The *T*-layer was initiated at the time when the detonation wave reached the nozzle throat of the MHD generator. The MHD duct 3.5 m in length had a constant opening angle $\alpha = 10°$ for each electrode. The electrodes were assumed to be continuous and having the ideal conductivity, connected to the constant loading $R^L$ (курсивом). At the duct outlet, a diffuser 0.5 m in length was posed with increasing the outlet cross-section by a factor of 1.5.

The computations were carried out on a uniform mesh with step $dx$ = 0.0025 m, and time step $dt = 2.5 \cdot 10^{-8}$ s. The radiation was taken into account in the range from $0.25 \cdot 10^6$ m$^{-1}$ to $150 \cdot 10^6$ m$^{-1}$; the spectrum was partitioned uniformly into five groups. For the high pressure generator $p_0$ = 30 atm, $B_0$ = 15 Tl, $R^L = 2 \cdot 10^{-3}$ Ohm, for the low pressure generator $p_0$ = 0.5 atm, $B_0$ = = 6 Tl, $R^L = 3 \cdot 10^{-2}$ Ohm.

Figure 2 shows the dynamics of

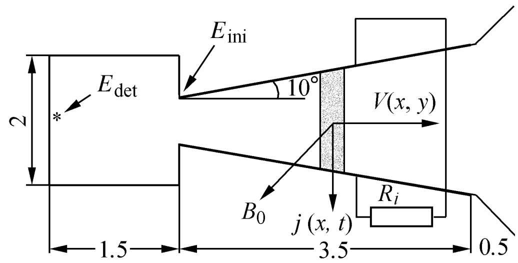


*Fig. 1* The scheme of detonation MHD generator. (На рисунке ошибка: $R_i$ нужно заменить на $R_L$) The dimensions in meters.

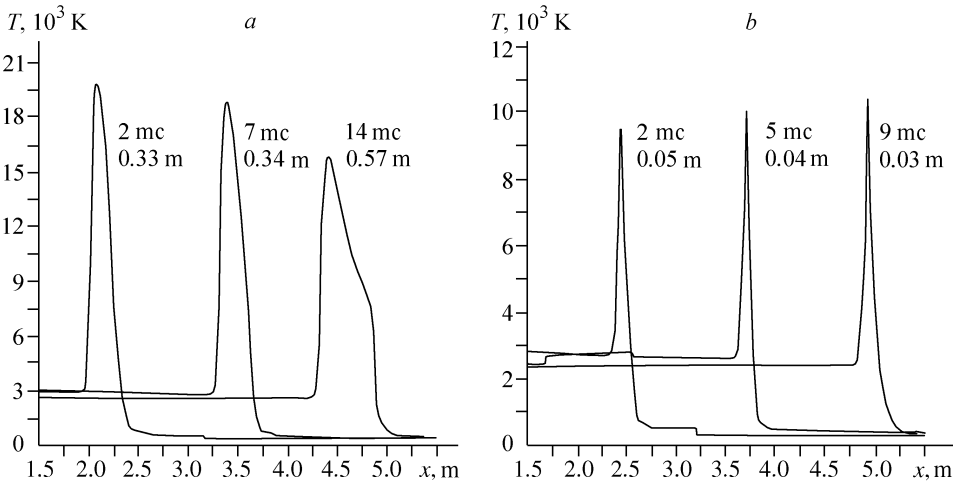


*Fig. 2.* The T-layer motion dynamics in the duct.
*a* is the high pressure generator; *b* is the low pressure generator.

the temperature profile variation of the *T*-layer at its motion in the MHD duct. It may be seen that in the high pressure generator (Fig. 2, *a*) the *T*-layer temperature reaches $2 \cdot 10^4$ K, and its effective width makes about 30 cm. In the low pressure generator (Fig. 2, *b*) the *T*-layer dimension is considerably smaller and amounts to 3 – 4 cm, and the temperature makes about $10^4$ K. The power characteristics of the processes of the interaction in the generators are given in Table 1.

If one adheres to the concept that the MHD duct width must be comparable with a reference size of the *T*-layer, then one can estimate the power of a unit duct as

$$W_{\text{el}} = \frac{E_L \tilde{\Delta l}}{T},$$

where $\tilde{\Delta l}$ is a dimensionless reference size of the *T*-layer. Then for the high pressure generator $W_{\text{el}} \cong 500$ MWt, and for low pressure generator $W_{\text{el}} \cong 1.0$ MWt. It should, however, be kept in mind that the MHD duct length cannot exceed the value of the order $20 \cdot \Delta l$ [5]. In other words, the high pressure duct length can reach 6 m (пробел между 6 и m), and for a low pressure duct it cannot exceed 1.0 m. The electric efficiency of a low pressure generator at such a length is negative.

Assuming that the duct length of a high pressure generator can be increased with regard for a reference size of the *T*-layer at least up to 6 m, one can expect that its effi-

**Table 1**

**Results of numerical experiments**

| Parameter | High pressure generator | Low pressure generator |
|---|---|---|
| $E_{\text{det}}$ | 271.5 MJ | 4.5 MJ |
| $E_{\text{ini}}$ | 15.0 MJ | 0.1 MJ |
| $E_{\text{dis}}$ | 18.2 MJ | 0.4 MJ |
| $E_L$ | 45.6 MJ | 0.3 MJ |
| $\eta$ *(вместо буквы был квадратик)* | 11 % | 5 % |
| $T$ | 18 ms | 9 ms |
| $W_L$ | 460 MWt/m$^3$ | 7 MWt/m$^3$ |

ciency will also increase at the expense of reducing the fraction of the initiation energy. The efficiency of the energy transformation into the electric power in the regime under study (with no regard for the initiation expenses) indeed amounts to 17 %. It is of course early to speak of a specific value of the electric efficiency, because the optimization of the electric and gas dynamic parameters of the generator is a subject of separate research.

The dependencies of loading currents $J(t)$ for high and low pressure generators are shown in Fig. 3. The effect of shock waves in the generator duct (in the form of current peaks) is observed in the dependence of current on time for the simplest electric scheme of generator and operation with purely ohmic loading. In the actual generator scheme the effect of shock waves will apparently decrease, however, they should be taken into account by virtue of the fact that they can either support or suppress the $T$-layer. Such regimes were observed in the course of numerical modeling.

With regard for the significance of the effect of characteristics of radiation from the $T$-layer on the formation of its structure and the efficiency of generator operation, the temperature profiles of $T$-layers of the high and low pressure generators were analyzed. In the first case, a temperature profile of the $T$-layer was chosen at the seventh millisecond of operation (the maximum temperature in the $T$-layer $T^{max}$ = = $1.9 \cdot 10^4$ K, the reference size $l$ = 34 cm, the pressure jump $p_1/p_2$ = 185 atm/45 atm). For a low pressure generator the temperature profile was considered at the fifth millisecond ($T^{max}$ = $10^4$ K, $\Delta l$ = 3 cm, $p_1/p_2$ = 3.5 atm/1.0 atm).

For an actual temperature profile of the $T$-layer and actual pressure jump the radiation fluxes towards the pushing gas $H_1$ and downstream to the generator outlet $H_2$, the corresponding brightness temperatures $T^b = \sqrt[4]{H/\sigma}$ and the blackness coefficients $\in = H/\sigma T^4$ were calculated. The computed results are shown in Fig. 4. For the high pressure generator $H_1 \cong 1.4 \cdot 10^8$ Wt/m$^2$, $H_2 \cong 2,7 \cdot 10^8$ Wt/m$^2$ (Вместо “|” нужно “·”) . The corresponding brightness temperatures are $7.1 \cdot 10^3$ K and $8.3 \cdot 10^3$ K, the blackness coefficients are 0.11 and 0.22. Since at the seventh millisecond the $T$-layer was in the duct region, where the duct height is equal to 1.2 m, the total radiation power may be estimated as $W_R = (H_1 + H_2)A = 4.76 \cdot 10^8$ Wt. If this power is accepted as a mean one, then

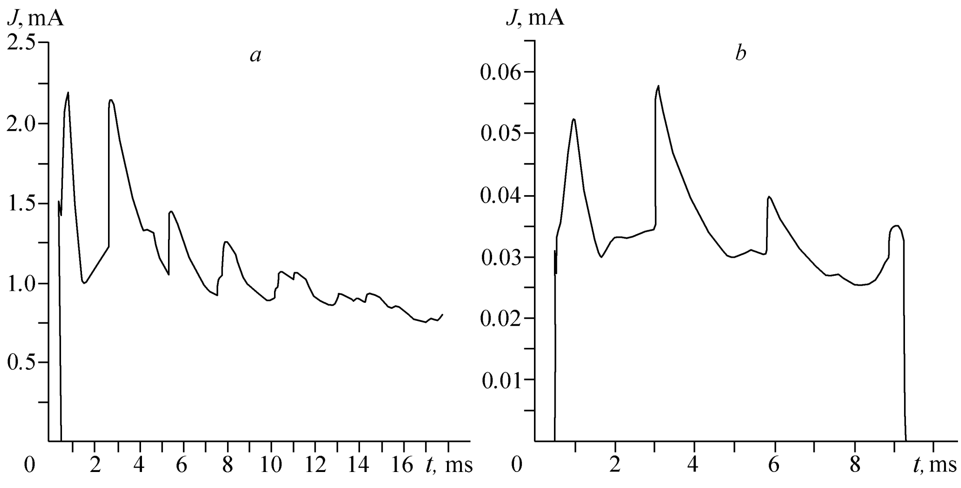


*Fig. 3*. The current momentum of the detonation MHD generator.
*a* is the high pressure generator; *b* is the low pressure generator.

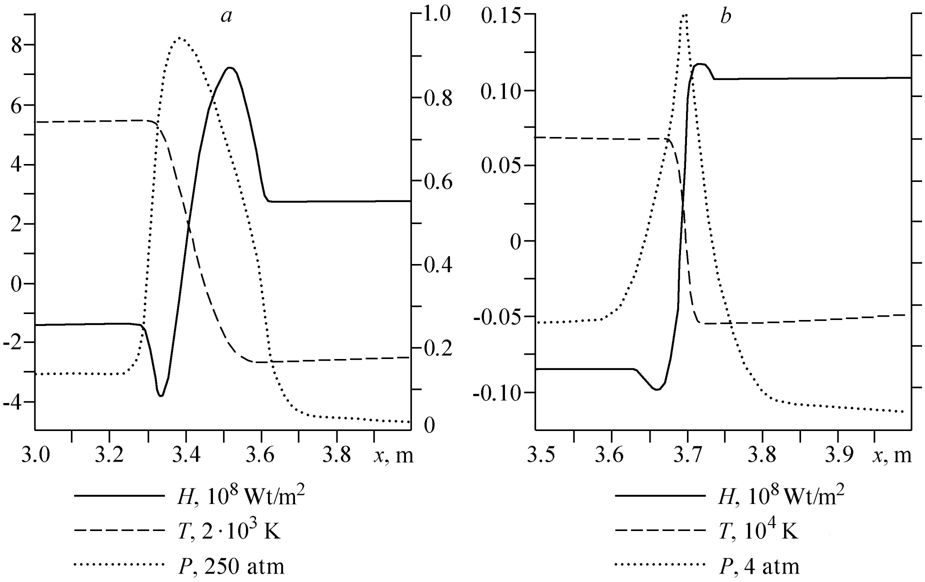


*Fig. 4*. The radiation flux from the *T*-layer.
*a* is the high pressure generator; *b* is the low pressure generator.

one can estimate the total radiation energy $E_R = W_R T = 7.4{\cdot}10^6$ J, which agrees quite satisfactorily with the radiation energy obtained at the numerical modeling (Fig. 5). For the low pressure generator $H_1 = 8.5{\cdot}10^6$ Wt/m$^2$, $H_2 = 10.7{\cdot}10^6$ Wt/m$^2$, the brightness temperature $3.5{\cdot}10^3$ K, the blackness coefficient 0.015 agree well with reference data.

Let us analyze the *T*-layer energy balance.

It was assumed previously in [6] that the *T*-layer structure stabilizes when the energy release at the expense of Joulean dissipation compensates for the radiation losses. Then it was shown in [7] for the low pressure generator that there is a *T*-layer drift opposite to the electrodynamic force action. It was found in [8] that the *T*-layer structure in

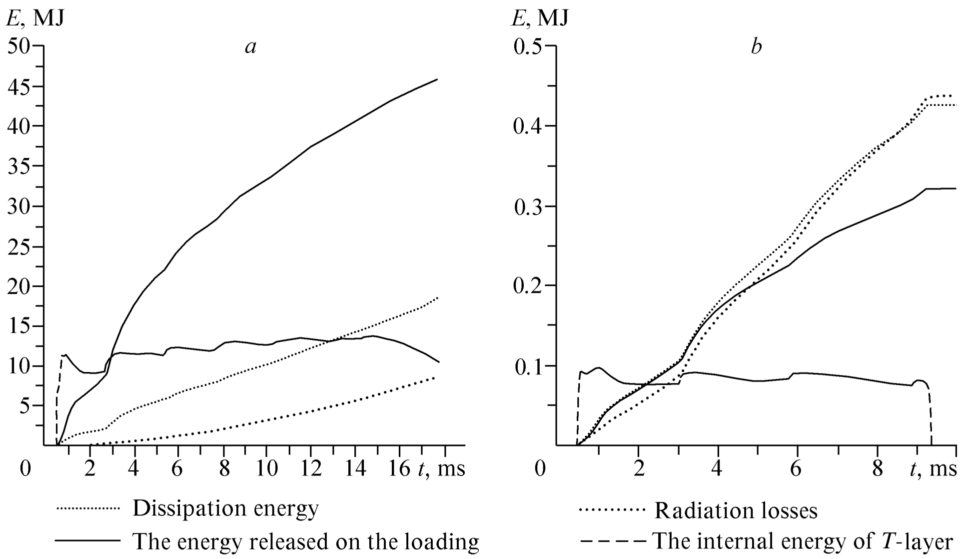


*Fig. 5*. The power characteristics of the detonation MHD generator.
*a* is high pressure generator; *b* is low pressure generator.

the high pressure generator changes abruptly, and a high temperature is settled in the high pressure region in the *T*-layer.

Figure 5 presents the power characteristics of high and low pressure generators. A pronounced excess of the Joulean dissipation energy over the radiation energy losses is revealed at the analysis of the energy balance of the high pressure generator under study. The assumption was made that the Joulean dissipation is spent also for increasing the internal energy of the *T*-layer and the heat and mass exchange with gas flow. In the high pressure region in the *T*-layer, where the maximum temperature is reached, the heating of pushing gas occurs, which leads to the increase in the *T*-layer internal energy. At the same time, the gas cooling occurs at the right boundary of the *T*-layer (downstream) at the expense of a considerably larger radiation flux. The gas loses its electric conductivity and moves to the rarefaction wave. Thus, the *T*-layer indeed moves upstream towards the electromagnetic deceleration force, and a part of the pushing gas flows through it. To analyze this phenomenon we have considered the variation of the energies of dissipation, radiation, and internal energy of the *T*-layer during the time from the second to the fifteenth milliseconds and computed the heat and mass exchange energy during this period of time:

$$E_{TME} = \Delta E_{\text{dis}} - \Delta E_R - \Delta E_{\text{layer}} .$$

The obtained results are presented in Table 2.

Thus, about 20 % of the Joulean dissipation energy are spent for the heat and mass exchange with the pushing gas flow and thereby characterizes the plasma piston “permeability”. The estimate of thermal power density across the *T*-layer gives the value 200 MWt/m$^2$.

In the low pressure generator the Joulean dissipation energy practically coincides with radiation energy, and there is practically no internal energy change after initiation. The detection of the effect of the heat and mass exchange of the *T*-layer with pushing gas flow by considering the power dependencies only has not met with success. The heat and mass exchange appears to lie outside the numerical experiment accuracy.

The computation of the *T*-layer internal energy shows that part of energy is spent at initiation for shock waves formation: immediately after initiation $E_{\text{layer}}$ reaches the value $13{\cdot}10^6$ J (Fig. 5, *a*) and makes 87 % of the energy spent.

## CONCLUSIONS

We note in concluding that the results of numerical experiments with a correct consideration of radiation and absorption in flow enable us to point to the impossibility of the development of a generator with the *T*-layer on the combustion products at low pressures. In the low pressure generator under consideration the loading coefficient did not exceed 0.4, that is the main part of the energy generated was spent for maintaining the *T*-layer. The attempts to increase the flow pressure (up to 10 atm) led to the *T*-layer disintegration. The results of high pressure generator investigation have lived up the expectations: the generator has a high specific power, a large loading coefficient (0.6 – 0.8), a

**Table 2**

**The estimate of the heat and mass exchange energy in the T-layer**

| Parameter | $E_{\text{dis}}$, MJ | $E_R$, MJ | $E_{\text{layer}}$, MJ | $E_{TME}$, MJ |
|---|---|---|---|---|
| $t$ = 2 ms | 1.68 | 0.005 | 9.08 | – |
| $t$ = 15 ms | 15.06 | 6.05 | 13.55 | – |
| $\Delta E$ | 13.38 | 6.05 | 4.47 | 2.86 |
| $\Delta E/\Delta E_{\text{dis}}$, % | 100 | 45.2 | 33.4 | 21.4 |

high electric efficiency, and a large reference size of the *T*-layer, which enables us to hope to develop an actual generator. The developed numerical model gives the possibility of obtaining a large amount of information about the generator operation, but it requires considerable computer time expenses for computations, and it should be improved for a detailed analysis of the operation regimes of the detonation MHD generator.

It is necessary to go over in subsequent research to the real gas equation of state and to optimize the gas dynamics of the duct flow, because the next emerging problem is the periodicity of generator operation. Just the generator periodicity will determine the possibility of the organization of a parametric regime of power generation.

**REFERENCES**


1. **V.A. Derevyanko and V.V. Derevyanko,** The model of detonation MHD generator with T-layer, TVT, 2000, Vol.. 6, P. 985 – 990.
2. **H.T. Huynh,** Accurate upwind methods for the euler equations, SIAM J. Numer. Anal., 1995, Vol. 32, No. 5, P. 1565 – 1619.
3. **B.N. Chetverushkin,** Mathematical Modeling of Problems of Radiating Gas Dynamics, Nauka, Moscow, 1985.
4. **E.N. Vasilyev, V.A. Derevyznko , and V.V. Ovchinnikov,** Radiation characteristics and structure of current layer in MHD channel, 10th Intern. Conf. on MHD Electric Power Generation. Dec. 4 – 8, Japan, 1989.
5. **E.N. Vasilyev, V.V. Ovchinnikov, V.V. Seredkina,** Thermophysical model of MHD-generator with *T*-layer, XI Intern. Conf. on MHD Electric Power Generation., Beijing, China, 1992.
6. **E.N. Vasilyev, V.A. Derevyanko, V.S. Slavin,** Stabilized current layer, TVT, 1986, Vol. 24, No. 5, P. 844 – 851.
7. **E.N. Vasilyev, V.S. Slavin, P.P. Tkachenko,** The effect of “sliding” of a discharge stabilized by the walls of the magnetogasdynamic duct, Prikl. Mekh. i Tekhn. Fiz., 1988, No. 4, P. 10.
8. **E.N. Vasilyev,** The current layer formation in conditions of radiation heat and mass exchange under high pressure, Izv. SO AN SSSR, Ser. Tehn. Nauk, 1990, No. 1, P. 94.